

Computational Optimal Control of the Saint-Venant PDE Model Using the Time-scaling Technique ¹

Tehuan Chen^a, Chao Xu^{a,2}

^a *State Key Laboratory of Industrial Control Technology and Institute of Cyber-Systems & Control, Zhejiang University, Hangzhou, Zhejiang 310027, China.*

Abstract

This paper proposes a new time-scaling approach for computational optimal control of a distributed parameter system governed by the Saint-Venant PDEs. We propose the time-scaling approach, which can change a uniform time partition to a nonuniform one. We also derive the gradient formulas by using the variational method. Then the method of lines (MOL) is applied to compute the Saint-Venant PDEs after implementing the time-scaling transformation and the associate costate PDEs. Finally, we compare the optimization results using the proposed time-scaling approach with the one not using it. The simulation result demonstrates the effectiveness of the proposed time-scaling method.

Keywords: Time-scaling approach, Optimal boundary control, Method of lines (MOL), Control parameterization method

1. Introduction

The one dimensional (1D) Saint-Venant (SV) model is a nonlinear hyperbolic system governed by quasilinear PDEs which can be obtained from the full Navier-Stokes equations (NSE) under certain assumptions and simplifications (i.e., [37, 17]). In hydraulics, the SV model is widely used to describe transient dam break analysis, open-channel flows and surface runoff. In addition, many phenomena arising in physical applications can be also modeled by the SV model, such as fluid flows in gas distribution pipeline

¹ This work was supported by the National Natural Science Foundation of China grants (61473253, 61320106009), the National High Technology Research and Development Program of China 2012AA041701, and Innovation Joint Research Center for Cyber-Physical-Society System.

² Correspondence to: Chao Xu, Email: cxu@zju.edu.cn

networks, open channel flows, multiphase flow in pipelines to transport crude oil over long distances (i.e., [36, 25]), just to name a few. In this work, we are interested in a boundary control problem of water hammer phenomenon while manipulating pipeline valves in large scale facilities for liquid distribution. Water hammer is also known as hydraulic shock which is a sharp pressure transition caused by changing the fluid motion state suddenly to halt or a reversed flow direction. This pressure wave could cause harmful effects to the hydraulic facilities, from noise and structural vibration to critical pipe component collapse. There are many applications for mitigation of water hammer, such as oil pipelines leakage [32], spacecraft propulsion systems [14], and even cardiovascular flow of blood vessels [21]. Therefore, passive mitigation methods are widely used to control water hammer, such as accumulators, expansion tanks and surge tanks [11]. The proposed strategy in the current work is to generate valve actuation command through computational optimization techniques based on the dynamic PDE model of water hammer, which can reduce the hydraulic shock as much as possible. Making boundary valves as active actuation could be an alternative or supplement to various passive protection measures.

Essentially, mitigation of water hammer using boundary valve actuation can be considered as a boundary stabilization problem in terms of the SV model in the point of view of PDE control. The characteristic method is one of the most important methods in the boundary control of SV model [3, 8]. There are mainly two streams of approaches of boundary stabilization of hyperbolic PDEs based on the characteristic method, including the Lyapunov functional method (e.g., [6, 28]) and the backstepping technique [13]. A strict Lyapunov function for hyperbolic systems of conservation laws is presented in [6] which can generate a boundary control law to guarantee the local convergence of the state towards a desired set point. The static feedback control law can be implemented as a feedback of the state only measured on the boundaries. A feedback control strategy is proposed in [28] which ensures that the water level and water flow can converge to the equilibrium exponentially. The backstepping technique has been extended to handle boundary stabilization of 2×2 hyperbolic linear and quasilinear PDEs, which allows L^2 -exponential convergence of the closed-loop and state estimation dynamics [7, 29]. Recently, a receding horizon optimal control (RHOC) for water hammer mitigation is

investigated for hydraulic pipeline systems described by the linearized SV model [22]. The approximate dynamic programming (ADP) framework is extended to a distributed parameter system described by a set of hyperbolic PDEs [12].

The current work considers a computational optimal control of the nonlinear SV model in contrast to a feedback stabilizing controller. Running the computational optimal control offline combined with an online tracking controller could be promising to realize a feedback controller for water hammer mitigation in practice. In general, there are mainly two categories of approaches to handle computational optimal control of infinite dimensional systems governed by PDEs, i.e., *discretize-then-optimize* (DTO) [35] and *optimize-then-discretize* (OTD) [27]. In the framework of DTO, PDEs are first discretized into finite dimensional systems governed by ODEs using various numerical methods, such as the finite volume method (FVM), the lattice Boltzmann method (LBM), and the method of lines (MOL). Then, classical computational techniques can be applied to solve the reduced optimal control problem, such as the control parameterization method, the time-scaling method and the exact penalty method [16, 15, 26, 18]. While in the framework of OTD, optimality conditions and gradient formula can be derived directly based on the PDEs and solve the coupled state and co-state PDEs using various numerical techniques [30].

In this paper, we extend the control parameterization method for finite dimensional control systems to an infinite dimensional system which is governed by the SV model (e.g., [26]). We developed a discretize-then-optimize computational approach for solving optimal control strategy of the SV model in [4]. This approach first uses the finite-difference method to approximate the PDE model by a system of ODEs, then applies control parameterization [26] to approximate the boundary control function. While in [5], we propose an alternative computational approach in which control parameterization is applied directly to the original SV model, then finite-difference methods are used to solve both the PDE model and costate equations. In both [4] and [5], the time partition used to parameterize the control input is equally divided. However, we realize that the control trajectory varies slop at different time instance and this motivates us to use less parameters for slowly changing segments but more for comparably fast changing ones. Therefore, we add a new optimization decision variable for the temporal step in

control parameterization. This allows us to adaptively select the best switching time instants, which result in a better control approximation. This ideal is called the time-scaling technique in the literature of computational optimal control of finite dimensional systems [26] but not complete for infinite dimensional systems governed by PDEs.

The rest of the paper is organized as follows. In Section 2, we state an optimal control problem for fluid flow during valve closure. In Section 3, the control parameterization method of the SV model using the time-scaling approach is applied to approximate the boundary control by piecewise linear functions. Then, it changes the boundary optimal problem to optimal parameter selection problem. In Section 4, we obtain the costate equations together with their boundary conditions as well as terminal conditions and the gradient formulas are derived by using the variational analysis method with respect to the control and time parameters. In Section 5, we use the MOL to compute the solutions of the state system and its costate system. Finally, we carry out numerical simulations to compare the control trajectories when the time-scaling approach is applied and not, respectively.

2. Statement of the Optimal Control Problem

The mathematical formulation of the optimal control problem with respect to the SV model can be stated as follows:

$$\min_u J(u(t)) = \frac{1}{T} \int_0^T \left[\frac{p(L, t) - P}{\bar{P}} \right]^{2\gamma} dt + \frac{1}{LT} \int_0^L \int_0^T \left[\frac{p(l, t) - P}{\bar{P}} \right]^{2\gamma} dt dl, \quad (1)$$

where $l \in [0, L]$ denotes the spatial, $t \in [0, T]$ is the time, γ is a positive integer, and \bar{P} is a given constant datum. The objective function (1) consists of two terms: the first term penalizes pressure fluctuation at the terminus while the second term penalizes pressure fluctuation at all points over the physical domain. Considering the actuator situated at terminal point which contains sensitive components that can be easily damaged, we place special emphasis at this point. The pressure drop $p(l, t)$ is the unique solution of

the following initial value problem

$$H_1(l, t) = \frac{\partial v(l, t)}{\partial t} + \frac{1}{\rho} \frac{\partial p(l, t)}{\partial l} + \frac{f v(l, t) |v(l, t)|}{2D} = 0, \quad (2a)$$

$$H_2(l, t) = \frac{\partial p(l, t)}{\partial t} + \rho c^2 \frac{\partial v(l, t)}{\partial l} = 0, \quad (2b)$$

$$p(l, 0) = \phi_1(l), \quad v(l, 0) = \phi_2(l), \quad l \in [0, L], \quad (2c)$$

where $v(l, t)$ is the flow velocity, $\phi_1(l)$ and $\phi_2(l)$ are given functions describing the initial state of the pipeline, D is the cross-sectional area, c is the wave velocity, f is the Darcy-Weisbach friction factor and ρ is the flow density which is usually considered as a constant. The benchmark model is shown in Figure 1, where a pipeline of length L is used to transport fluid from a reservoir to a terminus. Then the boundary conditions for system (2) are chosen as

$$p(0, t) = P, \quad (3a)$$

$$v(L, t) = u(t), \quad t \in [0, T], \quad (3b)$$

where P is the constant pressure generated by the reservoir which is very common in practice. $u(t)$ is a boundary control variable that models actuation such as a valve or water gate at the system terminus and subjected to the following constraints

$$u(0) = u_{\max}, \quad (4a)$$

$$u(T) = 0, \quad (4b)$$

where u_{\max} denotes the maximum velocity.

Remark 1. *Note that the open channel flows can be also modeled by the SV model. However, the variables of the flow are flow speed and water lever. This is different from the pressure pipe flow considered in this paper. For more information on open channel flows, please refer to [17].*

Problem P_0 . *Given the system (2a) (2b) with initial conditions (2c) and boundary conditions (3), choose the $u(t)$ with initial conditions (4a) to minimize the objective function (1) subject to the terminal control constraint (4b).*

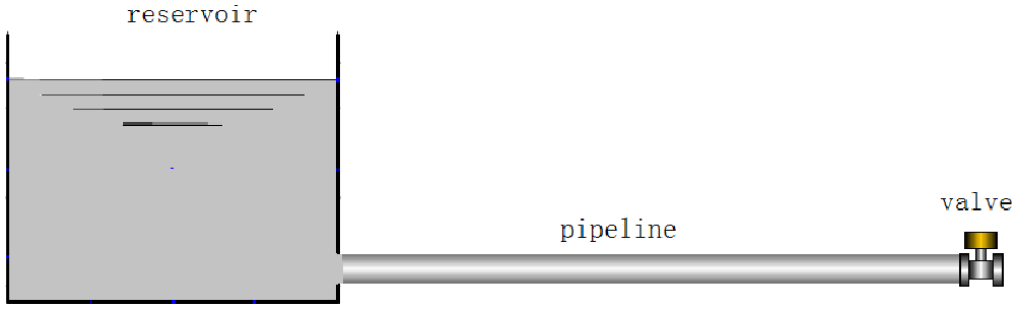


Figure 1: General layout of the pipeline system

3. Time-scaling Approach

By considering the flow rate is continuous, we can approximate the control signal $u(t)$ by piecewise-linear basis functions:

$$u(t) \approx \sum_{k=1}^r (\sigma_1^k t + \sigma_2^k) \chi_{[t_{k-1}, t_k)}(t), \quad (5)$$

where $\boldsymbol{\sigma}^k \triangleq \{\sigma_1^k, \sigma_2^k\} \in \mathbb{R}^2$, $k = 1, \dots, r$, are parameter vectors to be optimized and $\chi_{[t_{k-1}, t_k)}(t)$ is the indicator function defined by

$$\chi_{[t_{k-1}, t_k)}(t) = \begin{cases} 1, & \text{if } t \in [t_{k-1}, t_k), \\ 0, & \text{otherwise,} \end{cases} \quad (6)$$

and t_k , $k = 0, \dots, r$, are switching points such that

$$0 = t_0 < t_1 < t_2 < \dots < t_{r-1} < t_r = T. \quad (7)$$

Due to the continuity of flow rate, we have

$$\sigma_1^k t_k + \sigma_2^k = \sigma_1^{k+1} t_k + \sigma_2^{k+1}, \quad k = 1, \dots, r-1. \quad (8)$$

Furthermore, to ensure that the initial condition (4a) and terminal control constraint (4b) is satisfied (or the compatibility condition), we must have

$$\sigma_2^1 = u_{\max}, \quad \sigma_1^r T + \sigma_2^r = 0. \quad (9)$$

The time-scaling approach is to find the best temporal partition of each interval $[t_{k-1}, t_k]$, which means that we consider the switching points as the optimized parameters. However, switching time problem is difficult to solve, so we should transform it into a new

problem with fixed switching times [19]. Thus, the time-scaling function is defined as follows:

$$t(s) \triangleq \psi(s|\boldsymbol{\theta}) = \begin{cases} \sum_{k=1}^{\lfloor s \rfloor} \theta^k + \theta^{\lfloor s \rfloor+1}(s - \lfloor s \rfloor), & \text{if } s \in [0, r), \\ T, & s = r, \end{cases} \quad (10)$$

where $\lfloor s \rfloor$ donates an integer which is not larger than s . The relationship between t and s can be also defined through the following differential equation:

$$\begin{aligned} \frac{dt(s)}{ds} &= \sum_{k=1}^r \theta^k \chi_{[k-1, k)}(s), \quad s \in [0, r], \\ t(0) &= 0, \end{aligned} \quad (11)$$

where $\theta^k = t_k - t_{k-1}$ and $\theta^k > 0$.

We change the original time variable “ t ” into a new auxiliary variable “ s ”. Then the approximate piecewise-linear control (5) can be written as

$$u^r(s; \boldsymbol{\sigma}, \boldsymbol{\theta}) = \sum_{k=1}^r \left\{ \sigma_1^k \left(\sum_{k=1}^{\lfloor s \rfloor} \theta^k + \theta^{\lfloor s \rfloor+1}(s - \lfloor s \rfloor) \right) + \sigma_2^k \right\} \chi_{[k-1, k)}(s). \quad (12)$$

By denoting

$$\tilde{p}(l, s) = p(l, \psi(s|\boldsymbol{\theta})), \quad \tilde{v}(l, s) = v(l, \psi(s|\boldsymbol{\theta})), \quad (13)$$

the equation (2a) becomes

$$\begin{aligned} \dot{\tilde{v}}(l, s) &= \frac{\partial v(l, \psi(s|\boldsymbol{\theta}))}{\partial s} = \frac{\partial v(l, \psi(s|\boldsymbol{\theta}))}{\partial t} \frac{\partial \psi(s|\boldsymbol{\theta})}{\partial s} \\ &= \theta^k \left[-\frac{1}{\rho} \frac{\partial \tilde{p}(l, s)}{\partial l} - \frac{f \tilde{v}(l, s) |\tilde{v}(l, s)|}{2D} \right], \quad s \in (k-1, k), \quad k = 1, \dots, r, \end{aligned} \quad (14)$$

and the transformed form of (2b) can be obtained following the same procedure in deriving (14). Then the SV model becomes

$$H_1(l, s) = \frac{\partial \tilde{v}(l, s)}{\partial s} + \theta^k \frac{1}{\rho} \frac{\partial \tilde{p}(l, s)}{\partial l} + \theta^k \frac{f \tilde{v}(l, s) |\tilde{v}(l, s)|}{2D} = 0, \quad (15a)$$

$$H_2(l, s) = \frac{\partial \tilde{p}(l, s)}{\partial s} + \theta^k \rho c^2 \frac{\partial \tilde{v}(l, s)}{\partial l} = 0, \quad s \in (k-1, k), \quad k = 1, \dots, r, \quad (15b)$$

$$\tilde{p}(l, 0) = p(l, \psi(0|\boldsymbol{\theta})) = \phi_1(l), \quad \tilde{v}(l, 0) = v(l, \psi(0|\boldsymbol{\theta})) = \phi_2(l). \quad (15c)$$

Under the approximation (12) for the control input sequence, the objective function (1)

becomes

$$\begin{aligned}
J^r(\boldsymbol{\sigma}, \boldsymbol{\theta}) &= \frac{1}{T} \int_0^T \left[\frac{p^r(L, t) - P}{\bar{P}} \right]^{2\gamma} dt + \frac{1}{LT} \int_0^L \int_0^T \left[\frac{p^r(l, t) - P}{\bar{P}} \right]^{2\gamma} dt dl \\
&= \frac{1}{T} \sum_{k=1}^r \int_{t_{k-1}}^{t_k} \left[\frac{p^r(L, t) - P}{\bar{P}} \right]^{2\gamma} dt + \frac{1}{LT} \int_0^L \left\{ \sum_{k=1}^r \int_{t_{k-1}}^{t_k} \left[\frac{p^r(l, t) - P}{\bar{P}} \right]^{2\gamma} dt \right\} dl \\
&= \frac{1}{T} \sum_{k=1}^r \int_{\psi(k-1|\boldsymbol{\theta})}^{\psi(k|\boldsymbol{\theta})} \left[\frac{p^r(L, t) - P}{\bar{P}} \right]^{2\gamma} dt + \frac{1}{LT} \int_0^L \left\{ \sum_{k=1}^r \int_{\psi(k-1|\boldsymbol{\theta})}^{\psi(k|\boldsymbol{\theta})} \left[\frac{p^r(l, t) - P}{\bar{P}} \right]^{2\gamma} dt \right\} dl \\
&= \frac{1}{T} \sum_{k=1}^r \int_{k-1}^k \theta^k \left[\frac{\tilde{p}^r(L, s) - P}{\bar{P}} \right]^{2\gamma} ds + \frac{1}{LT} \int_0^L \left\{ \sum_{k=1}^r \int_{k-1}^k \theta^k \left[\frac{\tilde{p}^r(l, s) - P}{\bar{P}} \right]^{2\gamma} ds \right\} dl,
\end{aligned} \tag{16}$$

where $p^r(l, t)$, $\tilde{p}^r(l, s)$ denote the solution of system (2a) (2b) with $u(t) = u^r(t; \boldsymbol{\sigma})$ and system (15a) (15b) with $u(t) = u^r(s; \boldsymbol{\sigma}, \boldsymbol{\theta})$, respectively.

Moreover, we have the following linear constraint due to the fixed total time derivation of the valve operation process:

$$\theta_1 + \theta_2 + \cdots + \theta_r = T. \tag{17}$$

Then the continuity condition of the flow rate in (8) becomes following nonlinear constraints:

$$\sigma_1^k \sum_{m=1}^k \theta^m + \sigma_2^k = \sigma_1^{k+1} \sum_{m=1}^k \theta^m + \sigma_2^{k+1}, \quad k = 1, \dots, r-1. \tag{18}$$

Problem P_0^r . *Given the system (15a) (15b) with boundary conditions (3a) (12) and initial conditions (15c), choose the $u^r(s; \boldsymbol{\sigma}, \boldsymbol{\theta})$ to minimize the objective function (16) subject to the constraints (9), (17), (18).*

4. Gradient Computation

Problem P_0^r becomes a nonlinear programming problem. Since its gradient is an implicit function, we rewrite the objective function (16) and the variational method [2, 31, 20] is used to obtain the gradient formulas. The augmented objective function is

defined as

$$J^r(\boldsymbol{\sigma}, \boldsymbol{\theta}) = \frac{1}{T} \sum_{k=1}^r \int_{k-1}^k \theta^k \left[\frac{\tilde{p}^r(L, s) - P}{\bar{P}} \right]^{2\gamma} ds + \frac{1}{LT} \int_0^L \left\{ \sum_{k=1}^r \int_{k-1}^k \left\{ \theta^k \left[\frac{\tilde{p}^r(l, s) - P}{\bar{P}} \right]^{2\gamma} + \tilde{\lambda}(l, s) H_1(l, s) + \tilde{\mu}(l, s) H_2(l, s) \right\} ds \right\} dl, \quad (19)$$

where $\tilde{\lambda}(l, s)$, $\tilde{\mu}(l, s)$ are the Lagrangian multipliers and $H_1(l, s)$, $H_2(l, s)$ are defined in (15). Using integration by parts for (19), we can rewrite the objective function as

$$\begin{aligned} J^r(\boldsymbol{\sigma}, \boldsymbol{\theta}) &= \frac{1}{LT} \int_0^L \left\{ \sum_{k=1}^r \int_{k-1}^k \theta^k \left\{ \left[\frac{\tilde{p}^r(l, s) - P}{\bar{P}} \right]^{2\gamma} - \left[\frac{1}{\rho} \tilde{\lambda}_l(l, s) + \frac{\tilde{\mu}_s(l, s)}{\theta^k} \right] \tilde{p}^r(l, s) \right. \right. \\ &\quad \left. \left. + \tilde{\lambda} \left[\frac{f |\tilde{v}^r(l, s)|}{2D} - \frac{\tilde{\lambda}_s(l, s)}{\theta^k} - \rho c^2 \tilde{\mu}_l(l, s) \right] \tilde{v}^r(l, s) \right\} ds \right\} dl \\ &\quad + \frac{1}{T} \sum_{k=1}^r \int_{k-1}^k \theta^k \left\{ \left[\frac{\tilde{p}^r(L, s) - P}{\bar{P}} \right]^{2\gamma} + \frac{1}{L\rho} \left[\tilde{\lambda}(L, s) \tilde{p}^r(L, s) - \tilde{\lambda}(0, s) P \right] \right. \\ &\quad \left. + \frac{\rho c^2}{L} \left[\tilde{\mu}(L, s) u^r(s; \boldsymbol{\sigma}, \boldsymbol{\theta}) - \tilde{\mu}(0, s) \tilde{v}^r(0, s) \right] \right\} ds \\ &\quad + \frac{1}{LT} \int_0^L \left\{ \left[\tilde{\lambda}(l, r) \tilde{v}^r(l, r) - \tilde{\lambda}(l, 0) \phi_1(l) \right] + \left[\tilde{\mu}(l, r) \tilde{p}^r(l, r) - \tilde{\mu}(l, 0) \phi_1(l) \right] \right\} dl. \end{aligned} \quad (20)$$

Theorem 1. *The gradient formulas of the objective function with respect to the $\boldsymbol{\sigma} = [(\boldsymbol{\sigma}^1)^\top, \dots, (\boldsymbol{\sigma}^r)^\top]^\top$ and $\boldsymbol{\theta} = [\theta^1, \dots, \theta^r]^\top$ are given by*

$$\nabla_{\sigma_1^k} J(\boldsymbol{\sigma}, \boldsymbol{\theta}) = \frac{\rho c^2}{TL} \int_{k-1}^k \tilde{\mu}(L, s) \theta^k \left(\sum_{k=1}^{\lfloor s \rfloor} \theta^k + \theta^{\lfloor s \rfloor + 1} (s - \lfloor s \rfloor) \right) ds, \quad k = 1, \dots, r, \quad (21)$$

$$\nabla_{\sigma_2^k} J(\boldsymbol{\sigma}, \boldsymbol{\theta}) = \frac{\rho c^2}{TL} \int_{k-1}^k \tilde{\mu}(L, s) \theta^k ds, \quad k = 1, \dots, r, \quad (22)$$

$$\begin{aligned}
\nabla_{\theta^k} J(\boldsymbol{\sigma}) &= \frac{1}{LT} \int_0^L \left\{ \int_{k-1}^k \left\{ \left(\frac{\tilde{p}^r - P}{\bar{P}} \right)^{2\gamma} - \frac{1}{\rho} \tilde{\lambda}_l \tilde{p}^r + \left(\tilde{\lambda} \frac{f|\tilde{v}^r|}{2D} - \rho c^2 \tilde{\mu}_l \right) \tilde{v}^r \right\} ds \right\} dl \\
&+ \frac{1}{T} \int_{k-1}^k \left\{ \left[\frac{\tilde{p}^r(L, s) - P}{\bar{P}} \right]^{2\gamma} + \frac{1}{L\rho} \left\{ \tilde{\lambda}(L, s) \tilde{p}^r(L, s) - \tilde{\lambda}(0, s) P \right\} \right. \\
&+ \left. \frac{\rho c^2}{L} \tilde{\mu}(L, s) \left\{ \sigma_1^k \left[\sum_{m=1}^{\lfloor s \rfloor} \theta^k + \theta^{\lfloor s \rfloor + 1} (s - \lfloor s \rfloor) \right] + \sigma_2^k \right\} \right\} ds \\
&+ \frac{\rho c^2}{TL} \left\{ \sum_{m=k+1}^r \int_{m-1}^m \tilde{\mu}(L, s) \sigma_1^m \theta^m ds + \int_{k-1}^k \tilde{\mu}(L, s) \sigma_1^k \theta^k s ds \right\},
\end{aligned}$$

$$k = 1, \dots, r,$$

(23)

where $\tilde{\mu}(l, s)$ and $\tilde{\lambda}(l, s)$ can be solved from the following costate system

$$\begin{cases} \frac{2\gamma\theta^k}{\bar{P}} \left[\frac{\tilde{p}^r(l, s) - P}{\bar{P}} \right]^{2\gamma-1} - \frac{1}{\rho} \theta^k \frac{\partial \tilde{\lambda}(l, s)}{\partial l} - \frac{\partial \tilde{\mu}(l, s)}{\partial s} = 0, \\ \theta^k \tilde{\lambda} \frac{f|\tilde{v}^r(l, s)|}{D} - \frac{\partial \tilde{\lambda}(l, s)}{\partial s} - \theta^k \rho c^2 \frac{\partial \tilde{\mu}(l, s)}{\partial l} = 0, \\ \frac{1}{\rho} \tilde{\lambda}(L, s) + \frac{2\gamma L}{\bar{P}} \left[\frac{\tilde{p}^r(L, s) - P}{\bar{P}} \right]^{2\gamma-1} = 0, \\ \tilde{\mu}(0, s) = 0, \tilde{\lambda}(l, r) = \tilde{\mu}(l, r) = 0, \end{cases} \quad s \in [k-1, k), \quad k = 1, \dots, r.$$

(24)

Proof. By introducing the variational forms $\boldsymbol{\theta} + \epsilon \tilde{\boldsymbol{\theta}}, \boldsymbol{\sigma} + \epsilon \tilde{\boldsymbol{\sigma}}$, where ϵ is an arbitrarily positive constant, $\tilde{\boldsymbol{\theta}} = [\tilde{\theta}^1, \dots, \tilde{\theta}^r]^\top$, $\tilde{\boldsymbol{\sigma}} = [(\tilde{\sigma}^1)^\top, \dots, (\tilde{\sigma}^r)^\top]^\top$ are arbitrarily vectors chosen nontrivially, then (11) (12) change to

$$\frac{dt(s; \boldsymbol{\theta} + \epsilon \tilde{\boldsymbol{\theta}})}{ds} = \sum_{k=1}^r (\theta^k + \epsilon \tilde{\theta}^k) \chi_{[k-1, k)}(s), \quad s \in [0, r], \quad (25)$$

and

$$\begin{aligned}
&u^r(s; \boldsymbol{\sigma} + \epsilon \tilde{\boldsymbol{\sigma}}, \boldsymbol{\theta} + \epsilon \tilde{\boldsymbol{\theta}}) \\
&= \sum_{k=1}^r \left\{ (\sigma_1^k + \epsilon \tilde{\sigma}_1^k) \left(\sum_{m=1}^{\lfloor s \rfloor} (\theta^k + \epsilon \tilde{\theta}^k) + (\theta^{\lfloor s \rfloor + 1} + \epsilon \tilde{\theta}^{\lfloor s \rfloor + 1}) (s - \lfloor s \rfloor) \right) + \sigma_2^k + \epsilon \tilde{\sigma}_2^k \right\} \chi_{[k-1, k)}(s).
\end{aligned} \quad (26)$$

The corresponding perturbation for $\tilde{p}^r(l, s)$ and $\tilde{v}^r(l, s)$ are approximated as

$$\begin{aligned}\tilde{p}^r(l, s; \boldsymbol{\theta} + \epsilon \tilde{\boldsymbol{\theta}}, \boldsymbol{\sigma} + \epsilon \tilde{\boldsymbol{\sigma}}) &= \tilde{p}^r(l, s; \boldsymbol{\theta}, \boldsymbol{\sigma}) + \sum_{k=1}^r \langle \nabla_{\theta^k} \tilde{p}^r(l, s; \boldsymbol{\theta}, \boldsymbol{\sigma}), \epsilon \tilde{\theta}^k \rangle \chi_{[k-1, k)}(s) \\ &+ \sum_{k=1}^r \langle \nabla_{\sigma^k} \tilde{p}^r(l, s; \boldsymbol{\theta}, \boldsymbol{\sigma}), \epsilon \tilde{\sigma}^k \rangle \chi_{[k-1, k)}(s) + \mathcal{O}(\epsilon^2),\end{aligned}\tag{27}$$

$$\begin{aligned}\tilde{v}^r(l, s; \boldsymbol{\theta} + \epsilon \tilde{\boldsymbol{\theta}}, \boldsymbol{\sigma} + \epsilon \tilde{\boldsymbol{\sigma}}) &= \tilde{v}^r(l, s; \boldsymbol{\theta}, \boldsymbol{\sigma}) + \sum_{k=1}^r \langle \nabla_{\theta^k} \tilde{v}^r(l, s; \boldsymbol{\theta}, \boldsymbol{\sigma}), \epsilon \tilde{\theta}^k \rangle \chi_{[k-1, k)}(s) \\ &+ \sum_{k=1}^r \langle \nabla_{\sigma^k} \tilde{v}^r(l, s; \boldsymbol{\theta}, \boldsymbol{\sigma}), \epsilon \tilde{\sigma}^k \rangle \chi_{[k-1, k)}(s) + \mathcal{O}(\epsilon^2),\end{aligned}\tag{28}$$

where $\mathcal{O}(\epsilon^2)$ denotes higher order terms such that $\mathcal{O}(\epsilon^2) \rightarrow 0$ as $\epsilon \rightarrow 0$, defining the new notation $\eta_1^k = \langle \nabla_{\theta^k} \tilde{p}^r(l, s; \boldsymbol{\theta}, \boldsymbol{\sigma}), \tilde{\theta}^k \rangle$, $\eta_2^k = \langle \nabla_{\sigma^k} \tilde{p}^r(l, s; \boldsymbol{\theta}, \boldsymbol{\sigma}), \tilde{\sigma}^k \rangle$ and $\omega_1^k = \langle \nabla_{\theta^k} \tilde{v}^r(l, s; \boldsymbol{\theta}, \boldsymbol{\sigma}), \tilde{\theta}^k \rangle$, $\omega_2^k = \langle \nabla_{\sigma^k} \tilde{v}^r(l, s; \boldsymbol{\theta}, \boldsymbol{\sigma}), \tilde{\sigma}^k \rangle$. Then, the perturbed augmented objective function takes the following form

$$\begin{aligned}J(\boldsymbol{\theta} + \epsilon \tilde{\boldsymbol{\theta}}, \boldsymbol{\sigma} + \epsilon \tilde{\boldsymbol{\sigma}}) &= \frac{1}{LT} \int_0^L \left\{ \sum_{k=1}^r \int_{k-1}^k (\theta^k + \epsilon \tilde{\theta}^k) \left\{ \left[\frac{\tilde{p}^r + \epsilon \eta_1^k + \epsilon \eta_2^k - P}{\bar{P}} \right]^{2\gamma} - \left[\frac{1}{\rho} \tilde{\lambda}_l + \frac{\tilde{\mu}_s}{(\theta^k + \epsilon \tilde{\theta}^k)} \right] (\tilde{p}^r + \epsilon \eta_1^k + \epsilon \eta_2^k) \right. \right. \\ &+ \left. \left[\tilde{\lambda} \frac{f |(\tilde{v}^r + \epsilon \omega_1^k + \epsilon \omega_2^k)|}{2D} - \frac{\tilde{\lambda}_s}{\theta^k + \epsilon \tilde{\theta}^k} - \rho c^2 \tilde{\mu}_l \right] (\tilde{v}^r + \epsilon \omega_1^k + \epsilon \omega_2^k) \right\} ds \Bigg\} dl \\ &+ \frac{1}{T} \sum_{k=1}^r \int_{k-1}^k (\theta^k + \epsilon \tilde{\theta}^k) \left\{ \left[\frac{\tilde{p}^r(L, s) + \epsilon \eta_1^k(L, s) + \epsilon \eta_2^k(L, s) - P}{\bar{P}} \right]^{2\gamma} \right. \\ &+ \frac{1}{L\rho} \left\{ \tilde{\lambda}(L, s) \left[\tilde{p}^r(L, s) + \epsilon \eta_1^k(L, s) + \epsilon \eta_2^k(L, s) \right] - \tilde{\lambda}(0, s) P \right\} \\ &+ \frac{\rho c^2}{L} \left\{ \tilde{\mu}(L, s) \left\{ (\sigma_1^k + \epsilon \tilde{\sigma}_1^k) \left(\sum_{k=1}^{\lfloor s \rfloor} (\theta^k + \epsilon \tilde{\theta}^k) + (\theta^{\lfloor s \rfloor + 1} + \epsilon \tilde{\theta}^{\lfloor s \rfloor + 1})(s - \lfloor s \rfloor) \right) + \sigma_2^k + \epsilon \tilde{\sigma}_2^k \right\} \right. \\ &- \left. \left. \tilde{\mu}(0, s) \left[\tilde{v}^r(0, s) + \epsilon \omega_1^k(0, s) + \epsilon \omega_2^k(0, s) \right] \right\} \right\} ds \\ &+ \frac{1}{LT} \int_0^L \left\{ \left\{ \tilde{\lambda}(l, r) \left[\tilde{v}^r(l, r) + \epsilon \omega_1^k(l, r) + \epsilon \omega_2^k(l, r) \right] - \tilde{\lambda}(l, 0) \phi_1(l) \right\} \right. \\ &+ \left. \left\{ \tilde{\mu}(l, r) \left[\tilde{p}^r(l, r) + \epsilon \eta_1^k(l, r) + \epsilon \eta_2^k(l, r) \right] - \tilde{\mu}(l, 0) \phi_1(l) \right\} \right\} dl.\end{aligned}\tag{29}$$

By computing the derivative of $J(\boldsymbol{\theta} + \epsilon \tilde{\boldsymbol{\theta}}, \boldsymbol{\sigma} + \epsilon \tilde{\boldsymbol{\sigma}})$ with respect to the parameters ϵ , we

can obtain

$$\begin{aligned}
& \frac{dJ(\boldsymbol{\theta} + \epsilon \tilde{\boldsymbol{\theta}}, \boldsymbol{\sigma} + \epsilon \tilde{\boldsymbol{\sigma}})}{d\epsilon} \\
&= \frac{1}{LT} \int_0^L \left\{ \sum_{k=1}^r \int_{k-1}^k \tilde{\theta}^k \left\{ \left[\frac{\tilde{p}^r + \epsilon \eta_1^k + \epsilon \eta_2^k - P}{\bar{P}} \right]^{2\gamma} - \frac{1}{\rho} \tilde{\lambda}_l (\tilde{p}^r + \epsilon \eta_1^k + \epsilon \eta_2^k) \right. \right. \\
&\quad \left. \left. + \left[\tilde{\lambda} \frac{f |(\tilde{v}^r + \epsilon \omega_1^k + \epsilon \omega_2^k)|}{2D} - \rho c^2 \tilde{\mu}_l \right] (\tilde{v}^r + \epsilon \omega_1^k + \epsilon \omega_2^k) \right\} ds \right\} dl \\
&\quad + \frac{1}{LT} \int_0^L \left\{ \sum_{k=1}^r \int_{k-1}^k \left\{ \frac{2\gamma}{\bar{P}} (\theta^k + \epsilon \tilde{\theta}^k) \left[\frac{\tilde{p}^r + \epsilon \eta_1^k + \epsilon \eta_2^k - P}{\bar{P}} \right]^{2\gamma-1} - \left[\frac{1}{\rho} (\theta^k + \epsilon \tilde{\theta}^k) \tilde{\lambda}_l + \tilde{\mu}_s \right] \right\} (\eta_1^k + \eta_2^k) \right. \\
&\quad \left. + \left[(\theta^k + \epsilon \tilde{\theta}^k) \tilde{\lambda} \frac{f |(\tilde{v}^r + \epsilon \omega_1^k + \epsilon \omega_2^k)|}{D} - \tilde{\lambda}_s - (\theta^k + \epsilon \tilde{\theta}^k) \rho c^2 \mu_l \right] (\omega_1^k + \omega_2^k) \right\} ds \right\} dl \\
&\quad + \frac{1}{T} \sum_{k=1}^r \int_{k-1}^k \tilde{\theta}^k \left\{ \left[\frac{\tilde{p}^r(L, s) + \epsilon \eta_1^k(L, s) + \epsilon \eta_2^k(L, s) - P}{\bar{P}} \right]^{2\gamma} \right. \\
&\quad \left. + \frac{1}{L\rho} \left\{ \tilde{\lambda}(L, s) \left[\tilde{p}^r(L, s) + \epsilon \eta_1^k(L, s) + \epsilon \eta_2^k(L, s) \right] - \tilde{\lambda}(0, s) P \right\} \right. \\
&\quad \left. + \frac{\rho c^2}{L} \left\{ \tilde{\mu}(L, s) \left\{ (\sigma_1^k + \epsilon \tilde{\sigma}_1^k) \left(\sum_{k=1}^{\lfloor s \rfloor} (\theta^k + \epsilon \tilde{\theta}^k) + (\theta^{\lfloor s \rfloor+1} + \epsilon \tilde{\theta}^{\lfloor s \rfloor+1}) (s - \lfloor s \rfloor) \right) + \sigma_2^k + \epsilon \tilde{\sigma}_2^k \right\} \right. \right. \\
&\quad \left. \left. - \tilde{\mu}(0, s) \left[\tilde{v}^r(0, s) + \epsilon \omega_1^k(0, s) + \epsilon \omega_2^k(0, s) \right] \right\} \right\} ds \\
&\quad + \frac{1}{T} \sum_{k=1}^r \int_{k-1}^k (\theta^k + \epsilon \tilde{\theta}^k) \left\{ \frac{2\gamma}{\bar{P}} \left[\frac{\tilde{p}^r(L, s) + \epsilon \eta_1^k(L, s) + \epsilon \eta_2^k(L, s) - P}{\bar{P}} \right]^{2\gamma-1} \right. \\
&\quad \left. + \frac{1}{L\rho} \tilde{\lambda}(L, s) \right\} \left[\eta_1^k(L, s) + \eta_2^k(L, s) \right] \\
&\quad + (\theta^k + \epsilon \tilde{\theta}^k) \frac{\rho c^2}{L} \left\{ \tilde{\mu}(L, s) \left\{ \tilde{\sigma}_1^k \left(\sum_{k=1}^{\lfloor s \rfloor} (\theta^k + \epsilon \tilde{\theta}^k) + (\theta^{\lfloor s \rfloor+1} + \epsilon \tilde{\theta}^{\lfloor s \rfloor+1}) (s - \lfloor s \rfloor) \right) \right. \right. \\
&\quad \left. \left. + (\sigma_1^k + \epsilon \tilde{\sigma}_1^k) \left(\sum_{k=1}^{\lfloor s \rfloor} \tilde{\theta}^k + \tilde{\theta}^{\lfloor s \rfloor+1} (s - \lfloor s \rfloor) \right) + \tilde{\sigma}_2^k \right\} - \tilde{\mu}(0, s) \left[\omega_1^k(0, s) + \omega_2^k(0, s) \right] \right\} dt \\
&\quad + \frac{1}{LT} \int_0^L \left\{ \tilde{\lambda}(l, r) \left[\omega_1^k(l, r) + \omega_2^k(l, r) \right] + \tilde{\mu}(l, r) \left[\eta_1^k(l, r) + \eta_2^k(l, r) \right] \right\} dl.
\end{aligned} \tag{30}$$

By substituting $\epsilon = 0$, we can obtain

$$\begin{aligned}
& \left. \frac{dJ(\boldsymbol{\theta} + \epsilon \tilde{\boldsymbol{\theta}}, \boldsymbol{\sigma} + \epsilon \tilde{\boldsymbol{\sigma}})}{d\epsilon} \right|_{\epsilon=0} \\
&= \frac{1}{LT} \int_0^L \left\{ \sum_{k=1}^r \int_{k-1}^k \tilde{\theta}^k \left\{ \left[\frac{\tilde{p}^r - P}{\bar{P}} \right]^{2\gamma} - \frac{1}{\rho} \tilde{\lambda}_l \tilde{p}^r + \left[\tilde{\lambda} \frac{f|\tilde{v}^r|}{2D} - \rho c^2 \tilde{\mu}_l \right] \tilde{v}^r \right\} ds \right\} dl \\
&+ \frac{1}{LT} \int_0^L \left\{ \sum_{k=1}^r \int_{k-1}^k \left\{ \frac{2\gamma}{\bar{P}} \theta^k \left[\frac{\tilde{p}^r - P}{\bar{P}} \right]^{2\gamma-1} - \left[\frac{1}{\rho} \theta^k \tilde{\lambda}_l + \tilde{\mu}_s \right] \right\} (\eta_1^k + \eta_2^k) \right. \\
&+ \left. \left[\theta^k \tilde{\lambda} \frac{f|\tilde{v}^r|}{D} - \tilde{\lambda}_s - \theta^k \rho c^2 \mu_l \right] (\omega_1^k + \omega_2^k) \right\} ds \Big\} dl \\
&+ \frac{1}{T} \sum_{k=1}^r \int_{k-1}^k \tilde{\theta}^k \left\{ \left[\frac{\tilde{p}^r(L, s) - P}{\bar{P}} \right]^{2\gamma} + \frac{1}{L\rho} \left\{ \tilde{\lambda}(L, s) \tilde{p}^r(L, s) - \tilde{\lambda}(0, s) P \right\} \right. \\
&+ \left. \frac{\rho c^2}{L} \left\{ \tilde{\mu}(L, s) \left\{ \sigma_1^k \left(\sum_{k=1}^{\lfloor s \rfloor} \theta^k + \theta^{\lfloor s \rfloor+1} (s - \lfloor s \rfloor) \right) + \sigma_2^k \right\} - \tilde{\mu}(0, s) \tilde{v}(0, s) \right\} \right\} dt \\
&+ \frac{1}{T} \sum_{k=1}^r \int_{k-1}^k \theta^k \left\{ \frac{2\gamma}{\bar{P}} \left[\frac{\tilde{p}^r(L, s) - P}{\bar{P}} \right]^{2\gamma-1} + \frac{1}{L\rho} \tilde{\lambda}(L, s) \right\} \left[\eta_1^k(L, s) + \eta_2^k(L, s) \right] \\
&+ \theta^k \frac{\rho c^2}{L} \left\{ \tilde{\mu}(L, s) \left\{ \tilde{\sigma}_1^k \left(\sum_{k=1}^{\lfloor s \rfloor} \theta^k + \theta^{\lfloor s \rfloor+1} (s - \lfloor s \rfloor) \right) \right. \right. \\
&+ \left. \left. \sigma_1^k \left(\sum_{k=1}^{\lfloor s \rfloor} \tilde{\theta}^k + \tilde{\theta}^{\lfloor s \rfloor+1} (s - \lfloor s \rfloor) \right) + \tilde{\sigma}_2^k \right\} - \tilde{\mu}(0, s) \left[\omega_1^k(0, s) + \omega_2^k(0, s) \right] \right\} ds \\
&+ \frac{1}{LT} \int_0^L \left\{ \tilde{\lambda}(l, r) \left[\omega_1^k(l, r) + \omega_2^k(l, r) \right] + \tilde{\mu}(l, r) \left[\eta_1^k(l, r) + \eta_2^k(l, r) \right] \right\} dl.
\end{aligned} \tag{31}$$

The optimality condition to minimize objective function is to force $\delta J(u(t))$ to be zero. By using the fundamental lemma in the calculus of variation [31], one can obtain the costate system from (31) due to the arbitrary choice of $\tilde{\theta}$ and $\tilde{\sigma}$ in the variational form,

$$\begin{cases} \frac{2\gamma\theta^k}{\bar{P}} \left[\frac{\tilde{p}^r(l, s) - P}{\bar{P}} \right]^{2\gamma-1} - \frac{1}{\rho} \theta^k \frac{\partial \tilde{\lambda}(l, s)}{\partial l} - \frac{\partial \tilde{\mu}(l, s)}{\partial s} = 0, \\ \theta^k \tilde{\lambda}(l, s) \frac{f|\tilde{v}^r(l, s)|}{D} - \frac{\partial \tilde{\lambda}(l, s)}{\partial s} - \theta^k \rho c^2 \frac{\partial \tilde{\mu}(l, s)}{\partial l} = 0, \end{cases} \quad s \in [k-1, k), \quad k = 1, \dots, r, \tag{32}$$

where boundary conditions are

$$\begin{cases} \frac{1}{\rho} \tilde{\lambda}(L, t) + \frac{2\gamma L}{\bar{P}} \left[\frac{\tilde{p}^r(L, t) - P}{\bar{P}} \right]^{2\gamma-1} = 0, \\ \tilde{\mu}(0, s) = 0, \end{cases} \quad s \in [k-1, k), \quad k = 1, \dots, r. \tag{33}$$

The terminal time conditions at $s = r$ are

$$\tilde{\lambda}(l, r) = \tilde{\mu}(l, r) = 0. \quad (34)$$

By substituting (32)-(34) to (31), we can obtain

$$\begin{aligned} & \left. \frac{dJ(\boldsymbol{\theta} + \epsilon \tilde{\boldsymbol{\theta}}, \boldsymbol{\sigma} + \epsilon \tilde{\boldsymbol{\sigma}})}{d\epsilon} \right|_{\epsilon=0} \\ &= \frac{1}{LT} \int_0^L \left\{ \sum_{k=1}^r \int_{k-1}^k \tilde{\theta}^k \left\{ \left[\frac{\tilde{p}^r - P}{\bar{P}} \right]^{2\gamma} - \frac{1}{\rho} \tilde{\lambda}_l \tilde{p}^r + \left[\tilde{\lambda} \frac{f|\tilde{v}^r|}{2D} - \rho c^2 \tilde{\mu}_l \right] \tilde{v}^r \right\} ds \right\} dl \\ &+ \frac{1}{T} \sum_{k=1}^r \int_{k-1}^k \tilde{\theta}^k \left\{ \left[\frac{\tilde{p}^r(L, s) - P}{\bar{P}} \right]^{2\gamma} + \frac{1}{L\rho} \left\{ \tilde{\lambda}(L, s) \tilde{p}^r(L, s) - \tilde{\lambda}(0, s) P \right\} \right. \\ &+ \frac{\rho c^2}{L} \tilde{\mu}(L, s) \left\{ \sigma_1^k \left(\sum_{k=1}^{\lfloor s \rfloor} \theta^k + \theta^{\lfloor s \rfloor + 1} (s - \lfloor s \rfloor) \right) + \sigma_2^k \right\} \Bigg\} ds \\ &+ \frac{\rho c^2}{TL} \int_{k-1}^k \theta^k \tilde{\mu}(L, s) \left\{ \tilde{\sigma}_1^k \left(\sum_{k=1}^{\lfloor s \rfloor} \theta^k + \theta^{\lfloor s \rfloor + 1} (s - \lfloor s \rfloor) \right) + \sigma_1^k \left(\sum_{k=1}^{\lfloor s \rfloor} \tilde{\theta}^k + \tilde{\theta}^{\lfloor s \rfloor + 1} (s - \lfloor s \rfloor) \right) + \tilde{\sigma}_2^k \right\} ds. \end{aligned} \quad (35)$$

Therefore, we can obtain the following gradient formulas with respect to the optimization decision variable,

$$\nabla_{\sigma_1^k} J(\boldsymbol{\sigma}) = \frac{\rho c^2}{TL} \int_{k-1}^k \tilde{\mu}(L, s) \theta^k \left(\sum_{k=1}^{\lfloor s \rfloor} \theta^k + \theta^{\lfloor s \rfloor + 1} (s - \lfloor s \rfloor) \right) ds, \quad k = 1, \dots, r, \quad (36)$$

$$\nabla_{\sigma_2^k} J(\boldsymbol{\sigma}) = \frac{\rho c^2}{TL} \int_{k-1}^k \tilde{\mu}(L, s) \theta^k ds, \quad k = 1, \dots, r, \quad (37)$$

$$\begin{aligned} \nabla_{\theta^k} J(\boldsymbol{\sigma}) &= \frac{1}{LT} \int_0^L \left\{ \int_{k-1}^k \left\{ \left[\frac{\tilde{p}^r - P}{\bar{P}} \right]^{2\gamma} - \frac{1}{\rho} \tilde{\lambda}_l \tilde{p}^r + \left[\tilde{\lambda} \frac{f|\tilde{v}^r|}{2D} - \rho c^2 \tilde{\mu}_l \right] \tilde{v}^r \right\} ds \right\} dl \\ &+ \frac{1}{T} \int_{k-1}^k \left\{ \left[\frac{\tilde{p}^r(L, s) - P}{\bar{P}} \right]^{2\gamma} + \frac{1}{L\rho} \left\{ \tilde{\lambda}(L, s) \tilde{p}^r(L, s) - \tilde{\lambda}(0, s) P \right\} \right. \\ &+ \frac{\rho c^2}{L} \tilde{\mu}(L, s) \left\{ \sigma_1^k \left(\sum_{k=1}^{\lfloor s \rfloor} \theta^k + \theta^{\lfloor s \rfloor + 1} (s - \lfloor s \rfloor) \right) + \sigma_2^k \right\} \Bigg\} ds \\ &+ \frac{\rho c^2}{TL} \left\{ \sum_{m=k+1}^r \int_{m-1}^m \tilde{\mu}(L, s) \sigma_1^m \theta^m ds + \int_{k-1}^k \tilde{\mu}(L, s) \sigma_1^k \theta^k ds \right\}, \end{aligned}$$

$$k = 1, \dots, r.$$

(38)

□

5. Numerical Approximation

5.1. Simulation of the State System

Using the method of lines, which has been applied to obtain the numerical solution of the nonlinear SV model [1, 9], we can decompose the space domain into equally partitions $L_i = [l_{i-1}, l_i]$, $i = 1, \dots, N$, where N is an even integer with $l_0 = 0$ and $l_N = L$. Let $\tilde{v}_i^r(s) = \tilde{v}^r(l_i, s)$, $i = 0, \dots, N$, and $\tilde{p}_i^r(s) = \tilde{p}^r(l_i, s)$, $i = 0, \dots, N$. We make the following finite difference approximation scheme

$$\frac{\partial \tilde{p}_i^r(s)}{\partial l} = \frac{\tilde{p}_{i+1}^r(s) - \tilde{p}_i^r(s)}{\Delta l}, \quad i = 0, \dots, N-1, \quad (39a)$$

$$\frac{\partial \tilde{v}_i^r(s)}{\partial l} = \frac{\tilde{v}_i^r(s) - \tilde{v}_{i-1}^r(s)}{\Delta l}, \quad i = 1, \dots, N, \quad (39b)$$

where $\Delta l = L/N$. Then, we substitute the approximations (39a) and (39b) into the transformed dynamic system (15a) and (15b) to obtain the following finite dimensional representation

$$\dot{\tilde{v}}_i^r(s) = \theta^k \frac{1}{\rho \Delta l} (\tilde{p}_i^r(s) - \tilde{p}_{i+1}^r(s)) - \theta^k \frac{f \tilde{v}_i^r(s) |\tilde{v}_i^r(s)|}{2D}, \quad i = 0, \dots, N-1, \quad (40a)$$

$$\dot{\tilde{p}}_i^r(s) = \theta^k \frac{\rho c^2}{\Delta l} (\tilde{v}_{i-1}^r(s) - \tilde{v}_i^r(s)), \quad i = 1, \dots, N. \quad (40b)$$

For the initial conditions, we obtain

$$\tilde{p}^r(l, 0) = \phi_1(l_i), \quad \tilde{v}^r(l, 0) = \phi_2(l_i), \quad i = 0, \dots, N. \quad (41)$$

For the boundary conditions, we have

$$\tilde{p}_0^r(s) = P, \quad \tilde{v}_N^r(s) = u^r(s; \boldsymbol{\sigma}, \boldsymbol{\theta}). \quad (42)$$

Combining the transformed dynamic system (40) with the initial conditions (41) and the boundary conditions (42), we can numerically solve $\tilde{v}^r(l, s)$ and $\tilde{p}^r(l, s)$ forward in time.

5.2. Numerical Discretization of the Costate System

Similarly, the method of lines is also applied to solve the costate system (24) numerically. Let $\tilde{\lambda}_i(s) = \tilde{\lambda}(l_i, s)$, $i = 0, \dots, N$, and $\tilde{\mu}_i(s) = \tilde{\mu}(l_i, s)$, $i = 0, \dots, N$, and we can

obtain:

$$\dot{\tilde{\lambda}}_i(s) = \theta^k \tilde{\lambda}_i(s) \frac{f|\tilde{v}_i^r(s)|}{D} - \theta^k \rho c^2 \frac{\tilde{\mu}_{i+1}(s) - \tilde{\mu}_i(s)}{\Delta l}, \quad i = 0, \dots, N-1, \quad (43a)$$

$$\dot{\tilde{\mu}}_i(s) = \theta^k \frac{2\gamma}{\bar{P}} \left[\frac{\tilde{p}_i^r(s) - P}{\bar{P}} \right]^{2\gamma-1} - \theta^k \frac{1}{\rho} \frac{\tilde{\lambda}_i(s) - \tilde{\lambda}_{i-1}(s)}{\Delta l}, \quad i = 1, \dots, N. \quad (43b)$$

For the terminal conditions, we have

$$\tilde{\lambda}_i(r) = \tilde{\mu}_i(r) = 0, \quad i = 0, \dots, N. \quad (44)$$

For the boundary conditions, we obtain from (34)

$$\tilde{\mu}_0(s) = 0, \quad \tilde{\lambda}_N(s) = -\frac{2\rho L\gamma}{\bar{P}^{2\gamma}} [\tilde{p}_N^r(s) - P]^{2\gamma-1}. \quad (45)$$

With the terminal conditions (44) and the boundary conditions (45), and the values of $\tilde{p}_i^r(s)$ and $\tilde{v}_i^r(s)$, $i = 1, \dots, N$, obtained through solving (40), the approximate values of $\tilde{\lambda}(l, s)$ and $\tilde{\mu}(l, s)$ can be obtained by solving the system (43) backward in time. Moreover, we apply the composite Simpson's rule [10] to approximate the objective function (16) and its gradient formulas given by (21)-(23). For numerical integration, we divide each time interval into M subintervals. With the same integers N and M , we partition the space and time interval evenly to obtain the mesh points l_0, l_1, \dots, l_N and t_0, t_1, \dots, t_{rM} , where the step sizes $h = L/N$ and $\omega = T/(rM)$. Then, we can get the numerical integration of (16), (21), (22), (23).

5.3. Solving Problem P_0^r

To solve Problem P_0^r , computing the objective function (16) and its gradient (21)-(23) is the key point. Since we have already obtained the values of $\tilde{p}^r(l, s)$, $\tilde{v}^r(l, s)$, $\tilde{\lambda}(l, s)$ and $\tilde{\mu}(l, s)$, we can calculate the objective function and its gradient by applying the numerical integral approximation. Then, we can develop an effective gradient-based optimization technique, such as the SQP method, to solve Problem (P_0^r) numerically. The algorithm diagram is shown in Figure 2.

Note that Steps 4-5 can be implemented automatically by existing nonlinear optimization solvers, such as FMINCON in MATLAB.

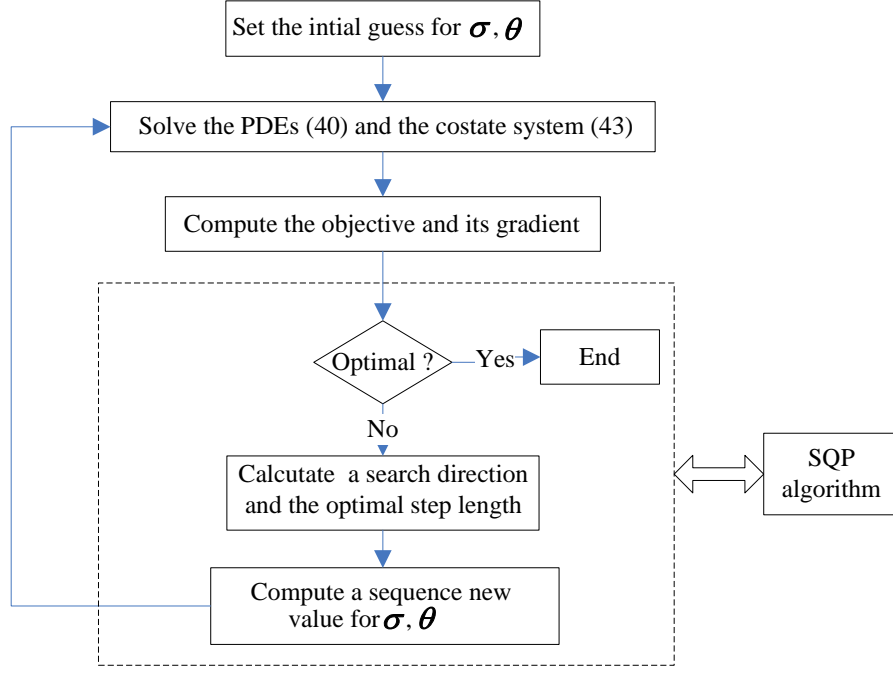


Figure 2: Gradient-based optimization framework for solving Problem P_0^c

6. Numerical Simulations

In this section, we will apply the proposed computational algorithm to an example to verify the effectiveness of the proposed method in this paper. The pipeline parameters are taken as: the total pipeline length $L = 100$ m, the diameter $D = 100$ mm, the flow density $\rho = 1000$ kg/m³, the wave speed $c = 1200$ m/s, the Darcy-Weisbach friction factor $f = 0.03$, $P = 2 \times 10^5$ Pa and $\bar{P} = 1 \times 10^5$ Pa. We also assume that the pipeline fluid flow is initially in the steady state with constant velocity $\phi_2(l_i) = 2$ m/s, $i = 0, \dots, N$. Then the initial pressure $\phi_2(l)$ is

$$\phi_2(l_i) = P - \frac{2\rho f}{D} l_i, \quad i = 0, \dots, N.$$

We set $N = 18$ for the spatial discretization of pipeline and choose $\gamma = 2$, $u_{\max} = 2$ m/s, $T = 10$ seconds. Our numerical simulation study was carried out within the MATLAB programming environment (version R2010b) running on a personal computer with the following configuration: Intel Core i5-2320 3.00GHz CPU, 4.00GB RAM, 64-bit Windows 7 Operating System.

We apply the proposed method to optimize the control sequence $\sigma_1^k, \sigma_2^k, \theta^k$, $k = 1, 2, \dots, r$. We also set the number of time segments $r = 10$ and the number of subinter-

Table 1: Optimal control parameters

k	1	2	3	4	5
σ_1^k	-0.4426	-0.3106	-0.2692	-0.1856	-0.1223
σ_2^k	2.0000	1.9108	1.8241	1.5972	1.3379
θ^k	0.6757	1.1493	0.6207	1.3797	0.6029
k	6	7	8	9	10
σ_1^k	-0.1528	-0.1544	-0.1383	-0.1478	-0.1334
σ_2^k	1.4811	1.4908	1.3866	1.4580	1.3343
θ^k	1.3668	0.4275	1.0306	1.0598	1.4169

vals $M = 100$. The optimal control parameters are given in Table 1. We compare the optimal control input curves in Figure 3 obtained by the time-scaling-based method and the time-scaling-free method, respectively. The objective values corresponding to the time-scaling-based method, time-scaling-free method and constant closure-rate method are 0.1163, 0.1512 and 0.4144, respectively. Obviously, the constant closure-rate method is worse than the other two methods. Figure 4 shows the corresponding pressure changes at the end of the pipeline ($l = L$) associated with valve actuation curves shown in Figure 3. The pressure evolutions along the pipeline according to both approaches are shown in Figure 5 and Figure 6, respectively. Clearly, result of the PDE-constraint optimization with the time-scaling approach is better than that without using the time-scaling approach. Using the time-scaling approach, we can change the uniform time interval into a nonuniform time interval. Then, computational optimized time interval will lead to smaller oscillations in the pressure evolution, which is shown in Figure 5 comparing to Figure 6.

7. Conclusion

In this paper, we proposed an effective computational method to design active optimal boundary control for the Saint-Venant model. The method of lines is used to

solve the state system and its costate system. From the numerical simulation, it is observed that result of PDE optimization with time-scaling approach is better than that of PDE optimization without using the time-scaling approach. In the future work, we can apply this method to output command tracking which has been studied in [23, 24] using the differential flatness approach of the simplified Hayami model. For real-time implementation of the proposed control method, we can use feedback control to track the optimal control target if the external perturbation is reasonably small. We can also carry out FPGA-based (Field Programmable Gate Array) implementation for real time optimization instead of software platform combined with model order reduction techniques [34, 33].

References

References

- [1] O. S. Balogun, M. Hubbard, and J. J. DeVries. Automatic control of canal flow using linear quadratic regulator theory. *Journal of Hydraulic Engineering*, 114(1):75–102, 1988.
- [2] Y. Cao, S. Li, L. Petzold, and R. Serban. Adjoint sensitivity analysis for differential-algebraic equations: The adjoint DAE system and its numerical solution. *SIAM Journal on Scientific Computing*, 24(3):1076–1089, 2003.
- [3] L. Cen, Y. Xi, D. Li, and Y. Cen. Boundary feedback control of open canals with a Riemann invariants approach. *Transactions of the Institute of Measurement and Control*, 37(7):900–908, 2015.
- [4] T. Chen, Z. Ren, C. Xu, and R. Loxton. Optimal boundary control for water hammer suppression in fluid transmission pipelines. *Computers and Mathematics with Applications*, 69(4):275–290, 2015.
- [5] T. Chen, C. Xu, Q. Lin, R. Loxton, and K. L. Teo. Water hammer mitigation via PDE-constrained optimization. *Control Engineering Practice*, accepted.

- [6] J. M. Coron, B. d’Andrea Novel, and G. Bastin. A strict Lyapunov function for boundary control of hyperbolic systems of conservation laws. *IEEE Transactions on Automatic Control*, 52(1):2–11, 2007.
- [7] J. M. Coron, R. Vazquez, M. Krstic, and G. Bastin. Local exponential H^2 stabilization of a 2×2 quasilinear hyperbolic system using backstepping. *SIAM Journal on Control and Optimization*, 51(3):2005–2035, 2013.
- [8] J. de Halleux, C. Prieur, J. M. Coron, B. d’Andréa Novel, and G. Bastin. Boundary feedback control in networks of open channels. *Automatica*, 39(8):1365–1376, 2003.
- [9] D. Georges. Nonlinear model identification and state-observer design for water distribution systems. In *Proceedings of IEEE International Conference on Control*, Coventry, UK, March 1994.
- [10] C. F. Gerald and P. O. Wheatley. *Numerical Analysis*. Addison-Wesley, 2003.
- [11] M. S. Ghidaoui, M. Zhao, D. A. McInnis, and D. H. Axworthy. A review of water hammer theory and practice. *Applied Mechanics Reviews*, 58(1/6):49–76, 2005.
- [12] M. Joy and N. S. Kaisare. Approximate dynamic programming-based control of distributed parameter systems. *Asia-Pacific Journal of Chemical Engineering*, 6(3):452–459, 2011.
- [13] M. Krstic and A. Smyshlyaev. *Boundary Control of PDEs: A Course on Backstepping Designs*. SIAM, 2008.
- [14] R. Lecourt and J. Steelant. Experimental investigation of waterhammer in simplified feed lines of satellite propulsion systems. *Journal of Propulsion and Power*, 23(6):1214–1224, 2007.
- [15] B. Li, C. Xu, K. L. Teo, and J. Chu. Time optimal Zermelo’s navigation problem with moving and fixed obstacles. *Applied Mathematics and Computation*, 224:866–875, 2013.

- [16] Q. Lin, R. Loxton, and K. L. Teo. The control parameterization method for nonlinear optimal control: A survey. *Journal of Industrial and Management Optimization*, 10(1):275–309, 2014.
- [17] X. Litrico and V. Fromion. *Modeling and Control of Hydrosystems*. Springer, 2009.
- [18] C. Liu, R. Loxton, and K. L. Teo. A computational method for solving time-delay optimal control problems with free terminal time. *Systems and Control Letters*, 72:53–60, 2014.
- [19] R. C. Loxton, K. L. Teo, and V. Rehbock. Optimal control problems with multiple characteristic time points in the objective and constraints. *Automatica*, 44(11):2923–2929, 2008.
- [20] S. J. Moura and H. K. Fathy. Optimal boundary control & estimation of diffusion-reaction PDEs. In *Proceedings of the 2011 American Control Conference*, San Francisco, USA, July 2011.
- [21] T. J. Pedley. *Fluid Mechanics of Large Blood Vessels*. Cambridge University Press, 1980.
- [22] V. Pham, D. Georges, and G. Besançon. Predictive control with guaranteed stability for water hammer equations. *IEEE Transactions on Automatic Control*, 59(2):465–470, 2014.
- [23] T. Rabbani, S. Munier, D. Dorchie, P. O. Malaterre, A. Bayen, and X. Litrico. Flatness-based control of open-channel flow in an irrigation canal using SCADA. *IEEE Transactions on Control Systems Technology*, 29(5):22–30, 2009.
- [24] T. S. Rabbani, F. Di Meglio, X. Litrico, and A. M. Bayen. Feed-forward control of open channel flow using differential flatness. *IEEE Transactions on Control Systems Technology*, 18(1):213–221, 2010.
- [25] P. Rao. Contribution of Boussinesq pressure and bottom roughness terms for open channel flows with shocks. *Applied Mathematics and Computation*, 133(2):581–590, 2002.

- [26] K. L. Teo, C. J. Goh, and K. H. Wong. *A Unified Computational Approach to Optimal Control Problems*. Longman Scientific and Technical, 1991.
- [27] F. Tröltzsch. *Optimal Control of Partial Differential Equations: Theory, Methods, and Applications*. American Mathematical Society, 2010.
- [28] D. S. Valérie and C. Prieur. Boundary control of open channels with numerical and experimental validations. *IEEE Transactions on Control Systems Technology*, 16(6):1252–1264, 2008.
- [29] R. Vazquez, M. Krstic, and J. M. Coron. Backstepping boundary stabilization and state estimation of a 2×2 linear hyperbolic system. In *Proceedings of the 50th IEEE Conference on Decision and Control and European Control Conference*. Orlando, USA, 2011.
- [30] Y. P. Wang and S. L. Tao. Application of regularization technique to variational adjoint method: A case for nonlinear convection–diffusion problem. *Applied Mathematics and Computation*, 218(8):4475–4482, 2011.
- [31] R. Weinstock. *Calculus of Variations*. Courier Dover Publications, 2012.
- [32] C. Xu, Y. Dong, Z. Ren, H. Jiang, and X. Yu. Sensor deployment for pipeline leakage detection via optimal boundary control strategies. *Journal of Industrial and Management Optimization*, 11(1):199–216, 2015.
- [33] C. Xu and E. Schuster. Low dimensional modeling of linear heat transfer systems using the incremental proper orthogonal decomposition method. *Asia-Pacific Journal of Chemical Engineering*, 8:473–482, 2013.
- [34] N. Yang, D. Li, J. Zhang, and Y. Xi. Model predictive controller design and implementation on FPGA with application to motor servo system. *Control Engineering Practice*, 20(11):1229–1235, 2012.
- [35] X. Yu, R. Cheng, H. Jiang, Q. Zhang, and C. Xu. The approximation for the boundary optimal control problem of Burgers–Fisher equation with constraints. *Applied Mathematics and Computation*, 243:889–898, 2014.

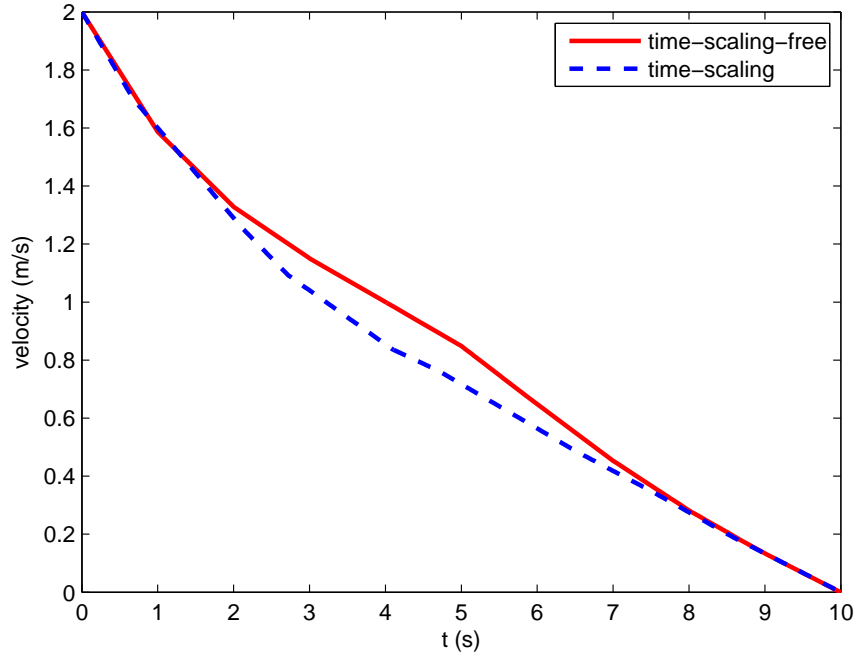


Figure 3: Optimal control curves with time scaling approach and without time scaling approach

- [36] S. Zhai, F. Yang, H. Yang, H. Ye, and G. Wang. Leak detection of gas pipelines based on wigner distribution. *Asia-Pacific Journal of Chemical Engineering*, 7(5):670–677, 2012.
- [37] J. G. Zhou. *Lattice Boltzmann Methods for Shallow Water Flows*. Springer, 2004.

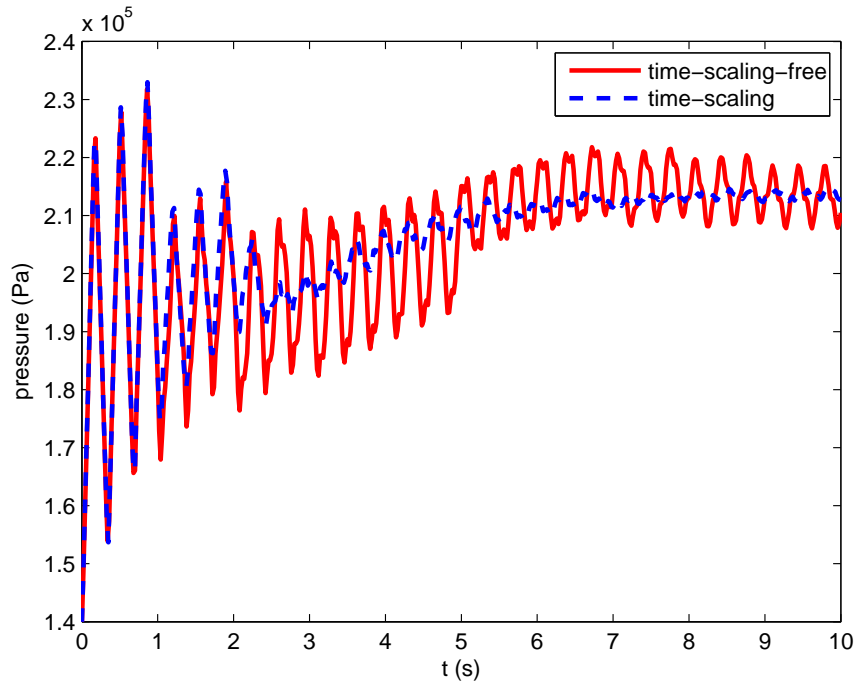


Figure 4: Comparison between PDE optimization with time scaling approach and without time scaling approach

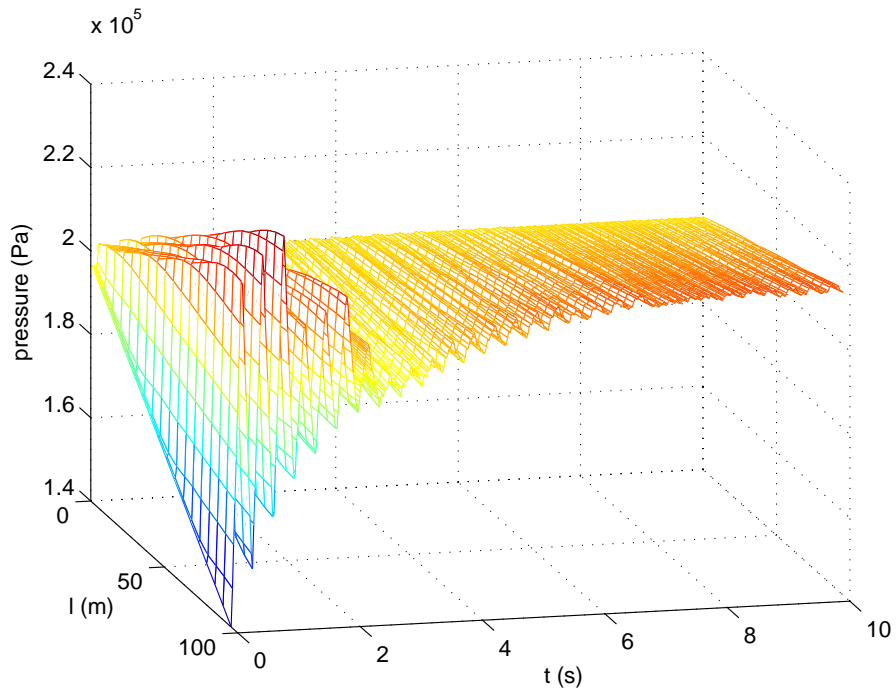


Figure 5: PDE optimization with time scaling approach

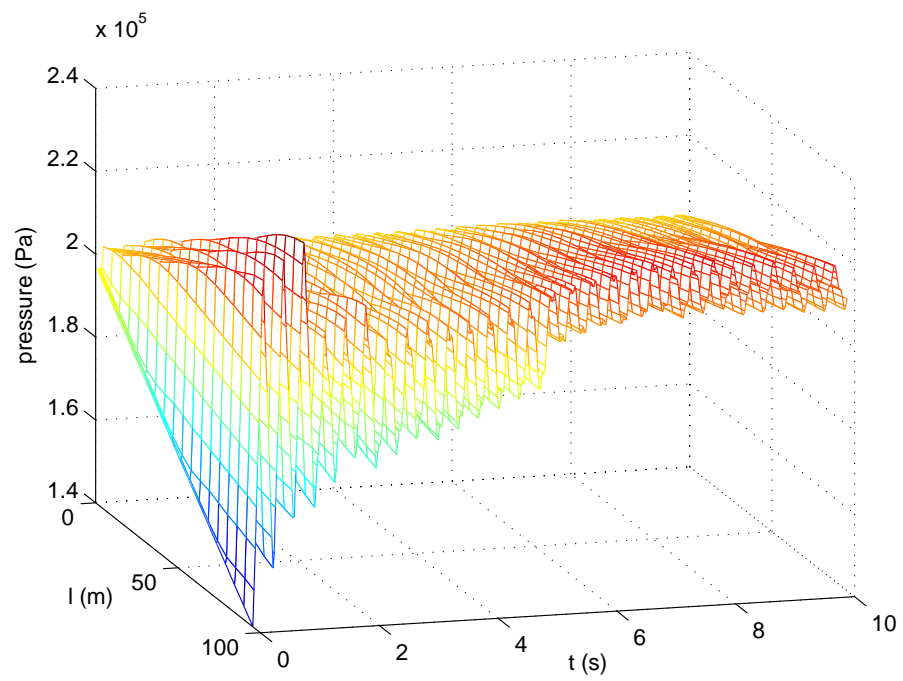


Figure 6: PDE optimization without time scaling approach